Fast Calculation of Cavity-Mode Characteristics of Photonic Crystal Cavities

Zexuan Qiang and Weidong Zhou, *Member, IEEE*

***Abstract*—A fast approach based on effective index perturbation method is proposed to evaluate the intrinsic characteristics of photonic-crystal-slab-based microcavity with two-dimensional finite-difference time-domain (2-D FDTD) technique. For two widely used single defect structures, less than 2% computational error was obtained in calculating the defect mode frequencies. Accurate prediction of cavity modal properties and resonant peak frequencies is feasible based on 2-D FDTD simulation by adjusting the effective index to match the dielectric band edge for donor-like defect mode. The correlation between the modified effective index and the cavity (lasing) mode with the highest quality factor Q offers an efficient tool in the design of defect mode based photonic crystal microcavities.**

***Index Terms*—Cavity quality factor, defect-mode cavity, effective index method (EIM), effective index perturbation (EIP), photonic crystal slabs (PCSs).**

I. Introduction

TWO-DIMENSIONAL (2-D) photonic-crystal-slab (PCS) microcavities have been a good candidate to perform single photon sources [1]–[3], biosensor [4], and high-sensitivity filter [5], due to their ultrasmall mode volume V, high quality factor Q, and enhanced spontaneous emission [6]. Significant progress has been made in the computational techniques for the design of PCS-based microcavity, and in the understanding of these cavity characteristics. Works reported to date are mostly based on three-dimensional (3-D) finite-difference time-domain (FDTD) technique [7]–[9], which can accurately simulate the characteristics of these devices. However, the fully vectorial 3-D FDTD approach is extremely time and computer memory consuming. The effective index method (EIM) [7], [10] has proved to be very effective and efficient in predicting the cavity properties with reduced dimensionality (from 3-D to 2-D), where only the effective index of fundamental guided mode of the unperturbed slab is considered. EIM is most effective for the low-index-contrast PCS. However, it becomes less accurate when it is applied to high index contrast PCSs, where high index contrast is favorable for reduced vertical cavity loss and better mode confinement. Efforts have been reported to adjust the effective index by matching the photonic band diagram (dispersion plot) with frequency offset [11] and effective index modification [12]. However, to the best of our knowledge, no work has been reported in EIM-based approaches, on the correlation of shifted photonic band diagram with the cavity defect mode and the corresponding quality factor Q.

In this letter, we introduce an effective index perturbation (EIP) technique in determining the suitable effective index for accurate prediction of cavity modal property and defect mode locations based on 2-D and 3-D plane-wave-expansion (PWE) techniques and the 2-D FDTD method. In donor-like defect mode cavities formed in air-column-based PCSs, very good agreement in defect mode locations was obtained with the EIP technique by matching the dielectric band edges simulated from 2-D and 3-D PWE techniques. The highest Q mode can also be correctly predicted, which is also very important in photonic crystal microcavity design, where the mode with the highest cavity Q could be most important in determining the cavity characteristics, including lasing and sensing.

II. Effective Index Perturbation

It is well-known that the air-band mode is more affected by removing an air hole and finally a donor state is excited and pulled into the bandgap from the air band [13]. In standard EIM, a relatively large error in predicting the resonant mode locations is often seen as a result of large offset in simulated photonic bandgap. This leads us to believe accurate prediction of resonant peak locations from 2-D FDTD is feasible by properly adjusting the effective index to matching the simulation photonic bandgaps. In this study, we found the suitable perturbation in effective index (n_{eff}) can lead to very small computation errors in resonant peak locations for these donor-like modes by matching the dielectric band edge. The procedure to choose the suitable n_{eff} is illustrated in Fig. 1. First, the dielectric band edge of 2-D PCS without defect f_d^{3D} is calculated by 3-D PWE. The standard effective refractive index of unperturbed slab waveguide is also done at this step by conventional methods [14]. Second, the 2-D PCS is transformed into an ideal 2-D PC structure with the high refractive index n_h replaced by the slab effective refractive index n_{eff}. The dielectric band edge of 2-D PC without defect f_d^{2D} is calculated by 2-D PWE. The calculated frequency error is computed as $\delta f = (f_d^{\text{2D}} - f_d^{\text{3D}})/f_d^{\text{3D}}$. If the value of δf is greater than 2%, an EIP is done to adjust the effective index n_{eff} based on δf (with sign): $n_{\text{eff}} = (1 + \delta f) \bullet n_{\text{eff}}$. Step 2 is repeated with perturbated n_{eff} until δf is less than 2%. Finally, we use the satisfied n_{eff} to calculate the quality factor and resonant wavelength by using the 2-D FDTD method in 2-D PCs with defect. Note that the criterion of 2% is set so that only one or two iterations are needed to get the accurate effective index. Higher accuracy with smaller tolerance could trans-

Manuscript received May 1, 2006; revised July 6, 2006. This work was supported by the Air Force Office of Scientific Research (AFOSR) under the SPRING and NANO Programs.

Z. Qiang is with the Nanofab Center, Department of Electrical Engineering, University of Texas at Arlington, Arlington, TX 75019-0072 USA, and also with the Institute of Optical Communication Engineering, Nanjing University, Nanjing 210093, China (e-mail: zxqiang@uta.edu).

W. Zhou is with the Nanofab Center, Department of Electrical Engineering, University of Texas at Arlington, Arlington, TX 75019-0072 USA (e-mail: wzhou@uta.edu).

Digital Object Identifier 10.1109/LPT.2006.882289

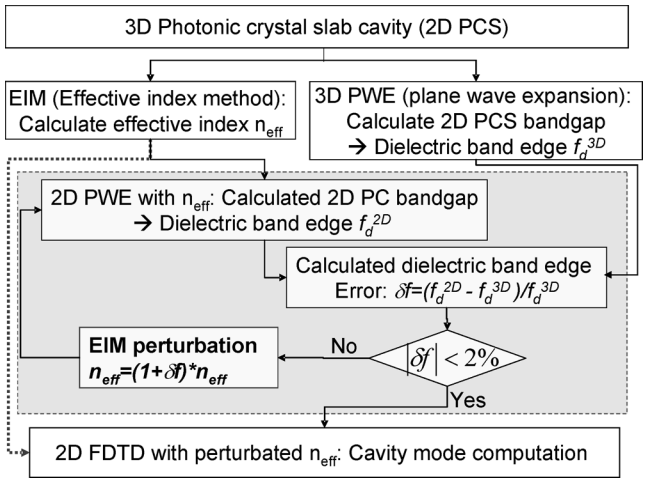

Fig. 1. Proposed procedure for accurate computation of photonic crystal defect-cavity resonant mode location based on EIP. Conventional EIM approach is shown with dashed lines.

late into more computation times with more iteration steps. It is also worth noting that in the process of finding proper n_{eff}, the defect-free structure can be used for 3-D and 2-D PWE-based bandgap calculations, which can greatly simplify the supercell construction, and thus reduce computation time. This is valid in the air-column-based photonic crystal structures with defect formed by removing/modifying the air hole sizes in the cavity region [13].

III. Simulation Results

Two-dimensional air-slab-air high index contrast PCS structures with single defect in the center of the air-column photonic crystals are considered here, as shown in the insets of Fig. 2. To validate the proposed EIP approach, simulations are done based on the structural parameters reported by Painter *et al.* [8] and Park *et al.* [9], where both 3-D FDTD simulation results as well as experimental results were reported for effective validation of our approach. In addition to the effective index obtained based on standard EIM (denoted as Case I in Fig. 3), three additional effective indexes were obtained by matching the photonic bandgap obtained from 2-D PWE with the photonic bandgap obtained from 3-D PWE, where matching criteria are set to be dielectric band edge (Case II), middle gap position (Case III), and air band edge (Case IV), respectively. The calculation errors for the bandgap position are calculated based on 2-D and 3-D PWE technique with different effective indexes (Cases I–IV). Note a large frequency offset (red-shift in the bandgap center frequency) is seen with standard EIM. It is mainly due to the fact that standard EIM approach only considers the slab without photonic crystals, which leads to an over-estimate in the effective index since the average index for the real slab is indeed smaller. Perturbation in effective index (reducing it in this case) should lead to better match in bandgap position and thus better match in resonant peaks. 2-D FDTD computation was carried out to find the defect mode locations and quality factors. The calculation error for the computed resonant peak locations for different effective indexes is derived by comparing the defect mode frequency simulated from 2-D FDTD (f_r^{2D}) to the frequency simulated based on 3-D FDTD (f_r^{3D}) with the following formula ($\delta f_r = (f_r^{\text{2D}} - f_r^{\text{3D}})/f_r^{\text{3D}}$). Only the defect mode with highest

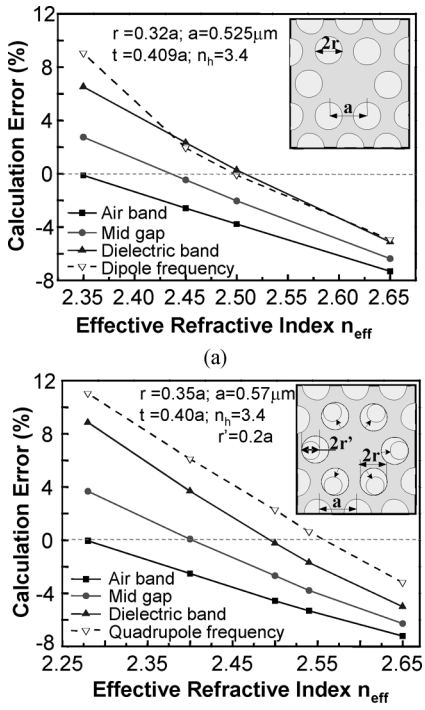

Fig. 2. Calculation errors for the bandgap and resonant frequencies with perturbated effective indexes in two different structures: (a) standard single defect cavity reported by Painter *et al.* [8]; (b) modified single defect cavity reported by Park *et al.* [9], where t is the slab thickness.

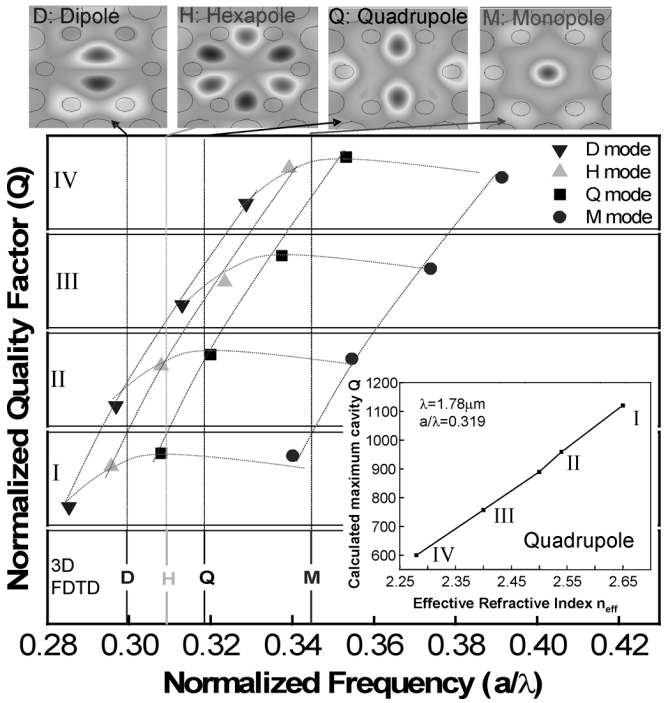

Fig. 3. Normalized quality factors for four different modes in the modified single defect cavity [Fig. 2(b)] for Cases I–IV, where the modal profiles are shown on top of the plot, along with the target frequencies based on 3-D FDTD simulation shown as the vertical dotted lines. The perturbated effective indexes are shown in the inset with the absolute cavity Q for the highest cavity Q mode (quadrupole mode in this case). A very good frequency match is seen for the quadrupole mode (the highest cavity Q mode) for Case II ($n_{\text{eff}} = 2.54$).

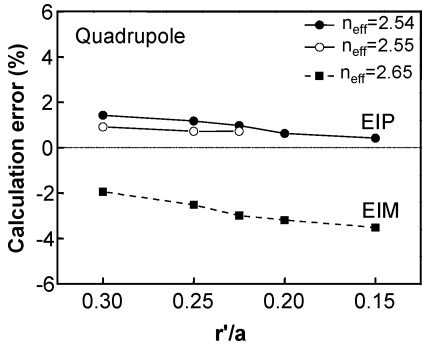

Fig. 4. Reduced calculation errors are plotted for modified single defect cavity structure shown in Fig. 2(b) with different inner hole radii (r'), based on standard EIM and proposed EIP approaches.

Q is shown in Fig. 2. Note very good agreement is obtained in the highest Q mode location ($\delta f_r < 2\%$) for Case IV, where the effective index is taken such that calculation error for the dielectric band edge is approaching zero.

In cases where multiple modes exist in the defect cavity, it is very important that the modal property does not change with the perturbation of effective index. Detailed modal property simulations were carried out for the structure shown in Fig. 2(b), where monopole (M), dipole (D), quadrupole (Q), and hexapole (H) coexist. The cavity mode profiles are shown on top of Fig. 3, with vertical dashed lines marking the corresponding defect mode locations based on 3-D FDTD simulations. The normalized Q values for different cavity modes are plotted for four Cases I–IV. Based on Fig. 3, it is seen (dotted lines connecting four different modes for each case) that the relative Q values (normalized to the maximum Q value at each case) remain unchanged for four different modes (M, Q, H, D), with quadrupole mode to be the highest Q mode for all cases. It can also be seen (dotted lines connecting the same modes at four cases with four different effective indexes) that all the modes within the cavity shift proportionally with respect to the bandgap positions. A very good match in the mode location is evident for Case II, where defect mode frequencies match to the target frequencies simulated from 3-D FDTD. In Case II, the effective index is adjusted to have dielectric band edge matched ($n_{\text{eff}} = 2.54$). It is also worth noting that the adjustment in effective index only changes the defect mode location and the absolute Q values. The absolute Q for the highest Q cavity mode (quadrupole as shown) is shown in the inset, where Q value increases with the increase of effective index.

Further validation is done by varying the radius r' for the structure shown in Fig. 2(b). Calculation errors for the quadrupole mode frequency are within 2% for perturbated effective index of 2.54 for different r'/a values (see Fig. 4). Further fine tuning is possible for even more accurate calculation in the resonant peak locations ($<1\%$ error), with better matched (dielectric) band edge.

IV. Conclusion

In summary, a fast 2-D approach to evaluate the cavity mode is proposed by using the EIP technique in combination with 2-D/3-D PWE techniques for bandgap simulation and 2-D FDTD for cavity mode location and Q simulation. The procedure can be used to accurately predict the cavity resonant frequency with highest cavity Q.

References

[1] O. Painter, R. K. Lee, A. Scherer, A. Yariv, J. D. O'Brien, P. D. Dapkus, and I. Kim, "Two-dimensional photonic bandgap defect mode laser," *Science*, vol. 284, pp. 1819–1821, Jun. 1999.

[2] J. K. Hwang, H. Y. Ryu, D. S. Song, I. Y. Han, H. K. Park, D. H. Jang, and Y. H. Lee, "Continuous room-temperature operation of optically pumped two-dimensional photonic crystal lasers at 1.6 μm," *IEEE Photon. Technol. Lett.*, vol. 12, no. 10, pp. 1295–7, Oct. 2000.

[3] W. D. Zhou, J. Sabarinathan, P. Bhattacharya, B. Kochman, E. Berg, P. C. Yu, and S. Pang, "Characteristics of a photonic bandgap single defect microcavity electroluminescent device," *IEEE J. Quantum Electron.*, vol. 37, no. 9, pp. 1153–1160, Sep. 2001.

[4] E. Chow, A. Grot, L. W. Mirkarimi, M. Sigalas, and G. Girolami, "Ultracompact biochemical sensor built with two-dimensional photonic crystal microcavity," *Opt. Lett.*, vol. 29, pp. 1093–1095, May 2004.

[5] Y. Akahane, M. Mochizuki, T. Asano, and S. Noda, "Design of a channel drop filter by using a donor-type cavity with high-quality factor in a two-dimensional photonic crystal slab," *Appl. Phys. Lett.*, vol. 82, pp. 1341–1343, Mar. 2003.

[6] M. Fujita, S. Takahashi, Y. Tanaka, T. Asano, and S. Noda, "Simultaneous inhibition and redistribution of spontaneous light emission in photonic crystals," *Science*, vol. 308, pp. 1296–1298, 2005.

[7] O. Painter, J. Vuckovic, and A. Scherer, "Defect modes of a two dimensional photonic crystal in optical microcavities," *J. Opt. Soc. Amer. B*, vol. 16, pp. 275–285, Feb. 1999.

[8] O. J. Painter, A. Husain, A. Scherer, J. D. O'Brien, I. Kim, and P. D. Dapkus, "Room temperature photonic crystal defect lasers at near-infrared wavelengths in InGaAsP," *J. Lightw. Technol.*, vol. 17, no. 11, pp. 2082–2088, Nov. 1999.

[9] H. G. Park, J. K. Hwang, J. Huh, H. Y. Ryu, S. H. Kim, J. S. Kim, and Y. H. Lee, "Characterization of modified single-defect two-dimensional photonic crystal lasers," *IEEE J. Quantum Electron.*, vol. 38, no. 10, pp. 1353–1365, Oct. 2002.

[10] M. Qiu, "Effective index method for heterostructure-slab-waveguide-based two-dimensional photonic crystals," *Appl. Phys. Lett.*, vol. 81, pp. 1163–1165, Aug. 2003.

[11] J. Witzens, M. Loncar, and A. Scherer, "Self-collimation in planar photonic crystals," *IEEE J. Sel. Topics Quantum Electron.*, vol. 8, no. 6, pp. 1246–1257, Nov./Dec. 2002.

[12] L. Yang, J. Motohisa, and T. Fukui, "Suggested procedure for the use of the effective-index method for high-index-contrast photonic crystal slabs," *Opt. Eng.*, vol. 44, pp. 078002-1–8, Jul. 2005.

[13] K. Ionue and K. Ohtaka, Eds., *Photonic Crystals: Physics, Fabrication and Applications*. Berlin, Germany: Springer Press, 2004.

[14] T. R. Graham and P. K. Andrew, *Silicon Photonics: An Introduction*. New York: Wiley, 2004.